



Original Article

Actin mesh in Re-epithelialization during skin regeneration in adult newt (*Cynops pyrrhogaster*)Yu Liou^a, Nobuko Moritoki^b, Tomoko Shindo^b, Tatsuyuki Ishii^{c,*}, Kazuo Kishi^{c,**}^a Department of Medical Education, Linkou Chang Gung Memorial Hospital, No.5, Fusing St., Gueishan Township, Taoyuan County 333, Taiwan^b Electron Microscope Laboratory, Keio University School of Medicine, Shinanomachi 35, Tokyo 160-8582, Japan^c Department of Plastic and Reconstructive Surgery, Keio University School of Medicine, Shinanomachi 35, Tokyo 160-8582, Japan

ARTICLE INFO

Article history:

Received 26 September 2024

Received in revised form

2 March 2025

Accepted 19 March 2025

Keywords:

Regeneration

Wound healing

Re-epithelialization

Actin

Newt

ABSTRACT

Introduction: Studies have highlighted the role of actin cables in embryonic scarless wound healing across various species. However, evidence for similar structures in adult animals remains lacking. Adult newts, known for their exceptional skin regeneration capabilities, are considered promising models for postnatal human studies. This study investigated actin fiber formation and alignment during re-epithelialization in the Japanese fire-bellied newt (*Cynops pyrrhogaster*).

Methods: Full-thickness skin excisions were performed, and actin structures were analyzed using immunohistochemistry and electron microscopy. The role of actin in re-epithelialization was assessed by inhibiting its formation with cytochalasin B. Myosin, an interacting cytoskeletal molecule, was examined through immunohistochemistry, while E-cadherin, an adhesion molecule, was analyzed using both immunohistochemistry and electron microscopy.

Results: Rather than an actin cable a mesh-like actin structure, termed the “actin mesh,” was identified via immunohistochemical analysis. The actin mesh developed alongside wound epidermis extension and disappeared following complete re-epithelialization. Inhibition of actin formation delayed re-epithelialization, although the overall healing process showed no significant difference from the control group. Immunohistochemistry revealed the presence of myosin II and E-cadherin alongside Filamentous actin. Electron microscopy further demonstrated actin-rich structures in the wound epidermis compared to normal skin and confirmed E-cadherin-mediated cell-cell adhesion in the wound area.

Conclusions: The actin mesh plays a critical role in facilitating rapid re-epithelialization in adult newts, presenting a valuable model for studying scarless wound healing in adult organisms. The involvement of interacting molecules such as myosin and E-cadherin provides insights into the underlying mechanisms of this process. This model offers potential applications for addressing intractable wounds in humans.

© 2025 The Author(s). Published by Elsevier BV on behalf of The Japanese Society for Regenerative Medicine. This is an open access article under the CC BY-NC-ND license (<http://creativecommons.org/licenses/by-nc-nd/4.0/>).

1. Introduction

Scarless wound healing has been pursued for decades because scar formation generally occurs after an injury or surgery. Physiological deformities can cause pain and other disadvantages and lead

to psychological disorders. Humans lose their skin regeneration capabilities after birth [1]. Fetal fibroblasts, which rapidly proliferate and synthesize type III collagen, undergo complete skin regeneration. However, the fetal fibroblasts are substituted by myofibroblasts in adulthood, expressing α -smooth muscle actin and leaving scars after wound healing. Although certain adult tissues, such as the oral mucosa and corneal epithelium, achieve scarless healing, these tissues are structurally simpler than skin. The oral mucosa lacks keratinization, while the cornea lacks vascularization, making their regenerative processes less complex than those required for full-thickness skin healing [2]. Similar to that in other mammals, scar-free regeneration occurs only during early gestation. However, some amphibians restore their capacity

This article is part of a special issue entitled: Future of Regenerative Medicine published in Regenerative Therapy.

* Corresponding author.

** Corresponding author.

E-mail addresses: ttsyksh@keio.jp (T. Ishii), kkishi@a7.keio.jp (K. Kishi).

Peer review under responsibility of the Japanese Society for Regenerative Medicine.

<https://doi.org/10.1016/j.reth.2025.03.014>

2352-3204/© 2025 The Author(s). Published by Elsevier BV on behalf of The Japanese Society for Regenerative Medicine. This is an open access article under the CC BY-NC-ND license (<http://creativecommons.org/licenses/by-nc-nd/4.0/>).

for regeneration, even in adulthood [2]. Among amphibians, the newt is the most favorable animal model for research because of its significant capacity for the regeneration of tissues and organs, such as the retina, brain, and limbs.

Research has revealed that adult newts have extraordinarily scarless wound-healing capabilities [3]. Complete skin regeneration with texture, appendages, and color recovery was observed after full-thickness skin excision, without granulation or fibrotic scarring. Notably, re-epithelialization began at the wound margin with a multilayered epidermis that rapidly covered the wound bed. Dermal reconstruction began after re-epithelialization, resulting in increased thickness and regeneration of skin appendages. Studies have tracked the epidermis around the wound margin during skin regeneration using transgenic fluorescent proteins and found that epithelial cells did not originate from the wound itself [3]. Instead, cell division occurred over a large area around the wound. In other words, the skin wound was closed by the overall expansion of the epidermis.

Actin cables are formed during wound regeneration in mammals [4]. The actin cable, which cooperates with myosin and other cytoskeleton proteins, forms a ring around the wound, facilitating a purse-string function in wound contractility. Cells are dragged from the margin of the wound by the circumferential force of the actin cable and finally overlay the wound bed when re-epithelialization is completed. This mechanism has been observed in the embryos of several species [5–10]. Therefore, we were curious whether the actin cable also participates in the healing process in adult newts.

In this study, we used the Japanese fire-bellied newt (*Cynops pyrrhogaster*) as an experimental animal because of its detailed description of skin regeneration, wound healing, and the availability of animal resources [3]. We hypothesized that *C. pyrrhogaster* generates actin cables for the contractility of the re-epithelialization process, and that a circular string structure of actin fibers could be observed around the wound. No cable or string structures formed by the actin were found. Instead, a net-like actin pattern, an actin mesh covering the wound bed was discovered during re-epithelialization.

2. Materials and methods

Experiments presented herein were performed at Keio University.

2.1. Animals

Sexually mature female Japanese fire-bellied newts, *C. pyrrhogaster*, were used in this study. They were captured from the Niigata, Fukui, and Ishikawa prefectures by a supplier (Aqua Grace, Yokohama, Japan) and stored at the University of Tsukuba. The animals were reared in plastic containers, in which the resting place (land) was provided in shallow water, at 18–22 °C under natural light conditions until experiments were performed [11]. Only healthy animals without visible wounds were selected for the experiments. The animals were then transported to Keio University and reared under the same conditions. The plastic containers were rinsed with running water twice weekly, and the paper towels used as resting places were replaced at the same frequency. Feed was provided immediately after the containers were cleaned. The feed was manufactured from Itosui. Co. Ltd with JAN code 4971453054017.

2.2. Anesthesia

FA100 (4-allyl-2-methoxyphenol; LF28C054; DS Pharma Animal Health, Osaka, Japan) was used as the anesthetic. Newts were anesthetized in 0.1 % FA100 dissolved in water in a capped bottle

(up to four newts in a total of 800 mL) at room temperature (RT: 22 °C) for 40 min to 1 h before taking pictures and performing surgical operations. In this protocol, newts awoke 1–2 h after anesthesia when placed at RT.

2.3. Surgical operations

Anesthetized animals were rinsed in distilled water (DW) and then dried on paper towels and placed under a dissecting microscope (M165 FC, Leica Microsystems, Wetzlar, Germany; SZX16, Olympus, Tokyo, Japan). Subsequently, using a microdissection blade, scissors, and forceps, a 4–9 mm² square-to-oval-shaped piece of full-thickness skin was carefully excised from one of the anterior limbs. Only one experimental wound was created on each animal to exclude the possible indirect influence of secondary or other wounds. Operated animals were momentarily placed on dry paper towels until the bleeding stopped and then transferred to moist containers with lids containing air vents (each newt per 150 mm × 50 mm × 50 mm container). The moist container was never filled with water but was always kept in a semi-dry condition. The bottom of the container was covered by a moist paper towel after it was tightly wrung, thereby providing folds or bumps on the surface of the crumpled towel that served as resting places for the wounded animals. The skin from each animal was allowed to regenerate in the moist containers at RT.

2.4. Preparation of tissue samples

At the desired time points for skin regeneration, the animals were anesthetized with 0.1 % FA100 dissolved in water for 40 min to 1 h. The middle of the upper arm was amputated and immediately transferred to a fixative. The animals were then transferred back to moist containers and allowed to regenerate and heal completely for use in other studies.

Samples were incubated in 4 % paraformaldehyde (PFA) in PBS at 4 °C for at least 6 h. After fixation, the tissue extending 5 mm from the wound margin was resected into a 3 mm slice. The cartilage was removed; however, the muscle under the wound bed remained intact to maintain the complete wound epithelium.

2.5. Staining tissue

The samples were washed twice with PBST, once with PBS, and blocked with 2 % bovine serum albumin (BSA) in PBS for 1 h at RT. For actin staining, the cells were incubated with Acti-stain 488 phalloidin (PHDG1-A, Cytoskeleton, Inc., 1:800) overnight at 5 °C. After washing twice with PBST and once with PBS, the nuclei were labeled with Cellstain DAPI Solution (FUJIFILM Wako Pure Chemical Co. Ltd. 1:500) and mounted on glass slides using ProLong Gold (Invitrogen). For immunostaining against E-cadherin and MyosinII, after blocking, primary antibodies rat anti-E-cadherin (SAB4200684, Sigma-Aldrich, St. Louis, 1:200) and rabbit anti-non-muscle MyosinIIb (ab230823, Abcam, 1:200) were diluted in a blocking solution (2 % BSA/PBS), and the tissue was incubated in antibody solution overnight at 4 °C. Then, the samples were washed twice with PBST, once with PBS, and incubated with the secondary antibody Alexa Fluor goat anti-rat IgG (ab150158, Invitrogen, Waltham, USA, 1:800) and goat anti-rabbit IgG (ab2535849, Invitrogen, Waltham, USA, 1:800), respectively, for 1 h at RT. The samples were washed twice with PBST and once with PBS and mounted on glass slides using ProLong Gold (Invitrogen). All slides were observed under a confocal laser scanning microscope (FLUOVIEW FV3000, Olympus Co. Ltd.).

2.6. Skin monitoring and image acquisition

Skin regeneration in live animals was monitored using a digital camera (EOS Kiss x7i, Canon, Tokyo, Japan, DP70, Olympus) attached to a dissecting microscope (M165 FC, Leica Microsystems, SZX16, Olympus). Transmitted light and fluorescence images of the tissue were acquired using a digital light microscope (BZ-X710, Keyence, Osaka, Japan) or a charge-coupled device (CCD) camera system (DP73, cellSens Standard 1.6, Olympus; DP22, cellSens Standard, Olympus) attached to a fluorescence microscope (BX50, Olympus).

2.7. Regulation of actin formation *in vivo*

After surgical excision, the newts were placed on a plastic platform with the wounded limb immersed in a 0.6 mL tube for 1 h at RT. Cytochalasin B (20 μ M) was used in the experiment group, with PBS: DMSO (500:1) as the control.

2.8. Scanning electron microscopy (SEM)

Skin wounds were cut into 9 mm squares for SEM observation, pre-fixed in 2.5 % glutaraldehyde/30 mM HEPES buffer (pH 7.4) for 16 h at 4 °C, and washed three times with 30 mM HEPES buffer for 20 min each. The tissue was post-fixed in 1 % osmium tetroxide/30 mM HEPES buffer for 2 h at 4 °C. The tissues were rinsed with DW and dehydrated with 50, 70, 80, 90, and 100 % ethanol for 30 min each. The tissues were then immersed in *t*-butyl alcohol three time for 20 min each, and frozen at –10 °C for 1 h. After that the frozen samples were dried in a freeze-drying equipment (VED-21S, Vacuum Devices, Inc., Japan). Samples were mounted on a specimen stand, ion sputter coated (SC-701, Sanyu-electron. Co., Japan) and observed under a scanning electron microscope (SU6600, Hitachi High-Tech Co., Japan).

2.9. Transmission electron microscopy (TEM)

Skin wounds were cut into 1 mm-thick sections for TEM observation. The sections were pre-fixed in 2.5 % glutaraldehyde/30 mM HEPES buffer (pH 7.4) for 16 h at 4 °C and washed three times with 30 mM HEPES buffer for 20 min each. The tissues were then post-fixed in 1 % osmium tetroxide/30 mM HEPES buffer (pH 7.4) for 2 h at 4 °C, rinsed with DW, and dehydrated in 50, 70, 80, 90, and 100 % ethanol for 30 min each. Next, the samples were immersed twice in *N*-butyl glycidyl ether (QY-1) twice for 30 min each, followed by several hours of penetration into a stepwise dilute mixture of QY-1 and epoxy resin mixtures. After several hours of penetration in the pure epoxy resin, the samples were embedded in the resin and polymerized at 60 °C, for 72 h. Samples were then sliced at a thickness of 70 nm using an ultramicrotome (UC7, Leica microsystems, Germany), stained with uranium acetate and lead staining solution, and observed with a transmission electron microscope (JEM-1400plus, JEOL Ltd., Japan).

3. Results

3.1. Actin mesh formation after full-thickness skin excision in adult *C. pyrrhogaster*

As observed in the previous studies done on the wound healing process in adult newts, wound epidermis developed within 24 h and became a tongue-like structure during extension under a dissecting microscope, termed “extending epidermal tongue (EET).” [3] Therefore, samples were collected 18 h after the full-thickness skin excision. EET was visible due to melanin pigmentation

within the epidermis (Fig. 1a). This structure was also observed using SEM. The wound epidermis was observed as a sheet extending from the wound margins. Weak attachment was observed between the wound epithelium and wound bed, as well as in the tissue sections. Therefore, the wound epidermis was curled at the margins (Fig. 1b).

Actin fibers were observed and evaluated using whole-mount phalloidin staining. No actin cables were observed, but interestingly, actin fibers were expressed in a reticular pattern only in the EET (Fig. 1c). Even when re-epithelialization was almost complete, mesh-like actin fibers were expressed only in EETs (Fig. 1d). During the re-epithelialization process, actin fibers formed abundantly around the cells and aligned as a mesh-like structure covering the wound bed. The tissue section 18 h after full-thickness skin excision demonstrated actin fibers twining the epithelial cells in the wound epidermis, whereas the unepithelialized wound bed showed no actin formation.

In addition, under TEM, fibers in the cytoplasm of the EET were much more abundant than in normal skin 12 h after surgical excision (Fig. 1e). Regardless of the distance from the wound margin, actin bundles were densely formed in the same manner in

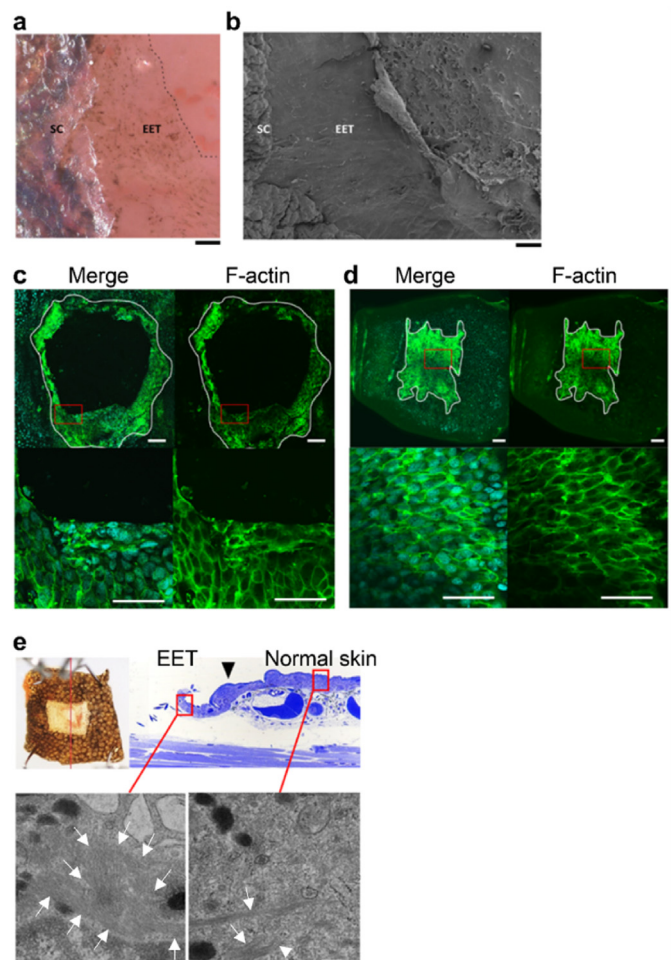


Fig. 1. Actin mesh formation after full-thickness skin excision in adult *C. pyrrhogaster*. (a) Optical microscope image of EET. (b) Electron microscope image of EET. (c) Fluorescent immunostaining of the wound after 18 h, showing mesh-like expression of F-actin in the EET. Green: F-actin; blue: DAPI. (d) Fluorescent immunostaining of the wound after 24 h. Re-epithelialization is almost complete. F-actin is strongly expressed throughout the wound epidermis. (e) Electron microscopic images of normal skin and EET. EET is actin-rich compared to normal skin. White arrows: actin fiber (a)–(d). Bar = 200 μ m, (e) Bar = 200 nm. EET: extending epidermal tongue; SC: stratum corneum; F-actin: filamentous actin.

all EET cells. The fact that EETs are markedly actin-rich compared with normal areas also supports the fact that actin mesh formation occurs during re-epithelialization.

3.2. Progression of the actin mesh formation

To understand the specific healing stages in which the actin mesh is involved, samples were collected at predetermined intervals corresponding to the morphological stages of skin regeneration in adult newts (Fig. 2) [3]. Upon excision of the full-thickness skin, re-epithelialization commenced, with the wound epidermis extending from the wound margins within 6–12 h at stage 2. During this initial phase, the actin mesh formed along the EET, contributing to the gradual central contraction of the wound. Subsequently, EET covered the wound bed, achieving complete re-epithelialization within 1–3 days at stage 3, during which the actin mesh densely enveloped the wound surface with tight weaves. From stage 4, 4–7 days postoperatively, while the dermal layer began to thicken from the wound margins, the actin mesh remained intact. Surprisingly, the persistent actin mesh did not dissipate as quickly as expected following the completion of re-epithelialization. Notably, the void observed at the wound margin during this stage was attributed to the uneven surface level of the skin. Shortly after the actin mesh was stabilized, melanophores and xanthophores located at the wound margin initiated migration, which played a pivotal role in restoring the pigment cell layer beneath the wound epidermis between days 7 and 14 at stage 5. Those pigment cells were visible only in tissue sections as a pigment layer under conventional staining but appeared dark in immunohistochemistry. This phase, characterized by cellular migration beneath the wound epidermis, coincided with a reduction in the actin mesh, which eventually reverted to a state resembling its pre-injury configuration.

3.3. Interference of actin mesh formation using cytochalasin B

The cytochalasin family comprises a group of natural organic molecules known for their direct interactions with actin during polymerization, making them invaluable tools for studying the role of actin in various biological processes [12]. In this study, we applied cytochalasin B locally by immersing a full-thickness skin excision wound in a cytochalasin B solution for 1 h (Fig. 3a). At 18 h post-operation, the control group exhibited a well-formed actin mesh across the EET, whereas the intervention group displayed minimal actin formation, lacking the characteristic net-like structure or the appearance of fibers (Fig. 3b). Despite these differences in actin organization, the wound areas in the intervention and control groups did not show significant differences within the first 24 h postoperatively. Both groups achieved complete re-epithelialization after 48 h. This indicates that actin meshes are transiently dysplastic due to cytochalasin B; however, this is not fatal for the outcome of re-epithelialization.

3.4. Interaction of actin mesh with cytoskeletal and adhesion molecules

In the early stages of wound healing, tensegrity describes the dynamic equilibrium between tension-generating and compression-bearing elements within the tissue [13]. Filamentous actin (F-actin) plays a crucial role in facilitating wound tension, whereas myosin generates the necessary contractility. Together, these molecules assemble into what is known as the actomyosin cable, which drives the purse-string force essential for wound closure. Immunofluorescence staining was performed to determine whether myosin contributed to newt re-epithelialization (Fig. 4a and b). The results showed that myosin II was aligned around the cells in the EET, mirroring the actin mesh distribution.

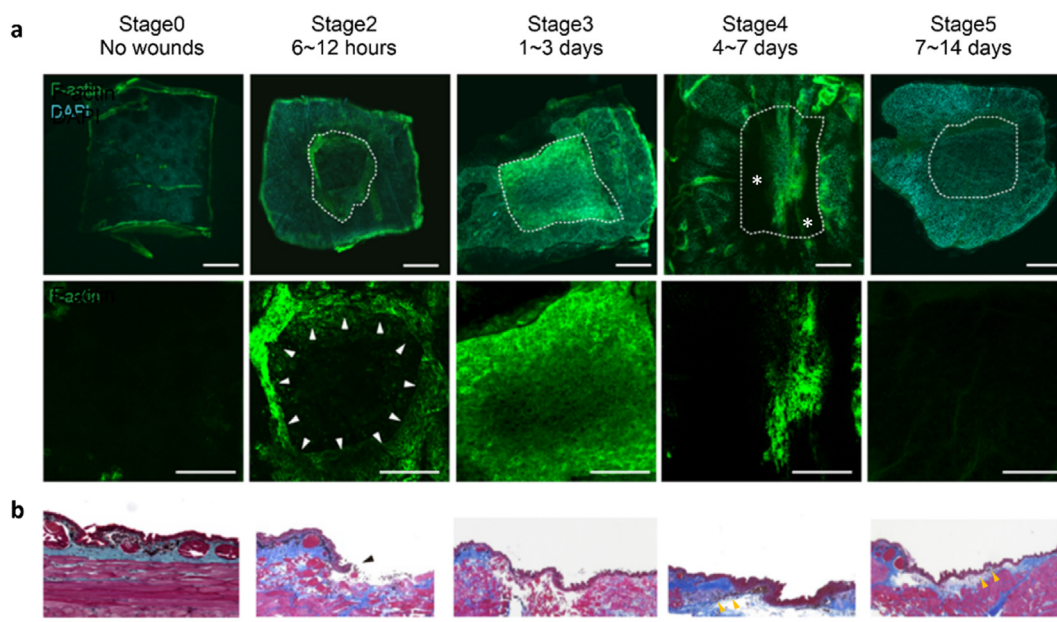


Fig. 2. Progression of the actin mesh formation. (a) Immunohistochemical analysis showing the time course of actin mesh development in the wound. At stage 1, no actin formation was observed in normal skin. At stage 2, actin fibers appeared in the wound epidermis. At stage 3, the actin mesh covered the wound bed, indicating complete re-epithelialization. At stage 4, the actin mesh persisted, with voids observed due to the uneven surface of the wound. At stage 5, the actin mesh disappeared. Green: F-actin; blue: DAPI. (b) Tissue sections stained with Masson's trichrome. Dotted line: wound margin; black and white arrows: leading edge of the wound epidermis; asterisks: voids; yellow arrow: pigment layer. Bar = 500 μ m.

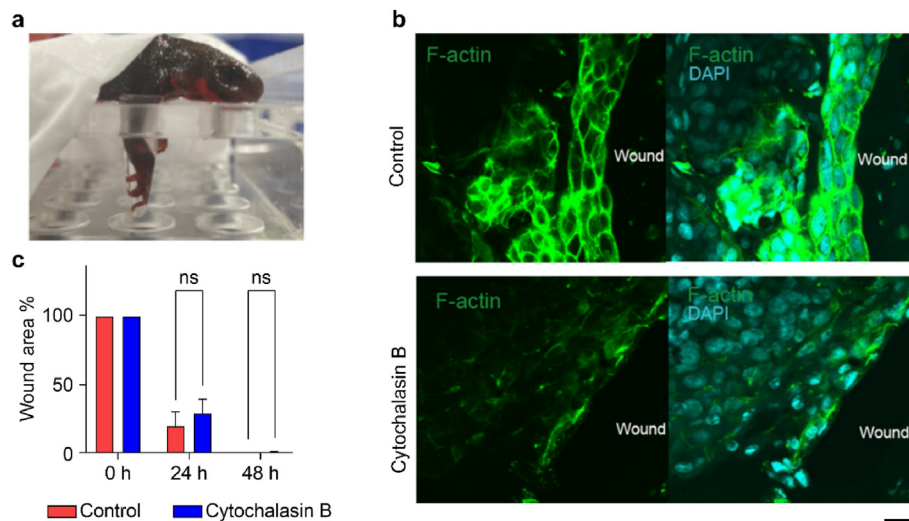


Fig. 3. Interference of actin mesh formation using cytochalasin B. (a) Immersion in cytochalasin B. (b) Effects of cytochalasin B on actin mesh. Actin mesh formation was prevented by cytochalasin B. Green: F-actin; blue: DAPI. (c) Comparison of wound area percentages in cytochalasin B-treated and control groups. No significant differences were found in epithelialization. $n = 3$. Bar = 20 μm .

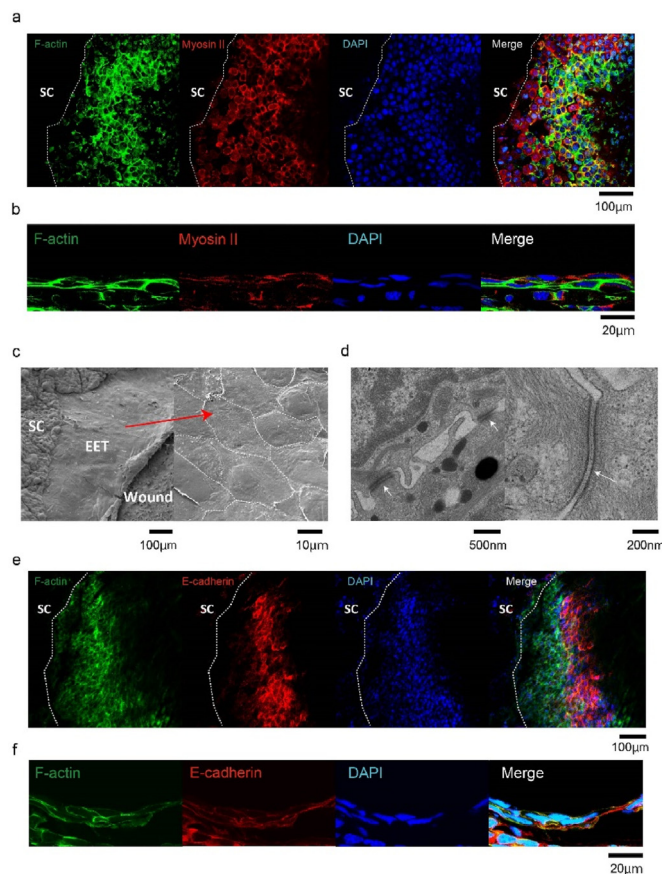


Fig. 4. Interaction of actin mesh with cytoskeletal and adhesion molecules. (a) (b) Fluorescence immunostaining images of F-actin and Myosin II during re-epithelialization process, in both whole-mount and transverse view. Green: F-actin; red: Myosin II; blue: DAPI. (c) SEM image of EET in the process of re-epithelialization. (d) TEM image of intercellular adhesion of EET. (e) (f) Fluorescence immunostaining images of F-actin and E-cadherin during re-epithelialization process, in both whole-mount and transverse view. Green: F-actin; red: E-cadherin; blue: DAPI. EET: extending epidermal tongue; SC: stratum corneum; F-actin: filamentous actin.

Another critical aspect of actin cable assembly is the role of intercellular adhesion molecules that link actin fibers between neighboring cells. These molecules are integral to maintaining tension across cells and guiding them toward the wound center [14]. In particular, E-cadherin acts as a core component of the adhesion junctions for actin assembly and serves as an anchor for actin cables [15]. Studies on fetal mice have reported E-cadherin expression following the appearance of the actin cables at the wound edge [5], suggesting that the actin cables are partially anchored to the cell membrane by E-cadherin. To further investigate E-cadherin expression in the actin mesh, we first performed SEM analysis of the samples (Fig. 4c). Magnified EET images revealed a scale-like pattern, indicating the presence of a potential actin mesh structure beneath the newly formed epidermis. Furthermore, under TEM at higher magnification, cells within the wound epidermis were connected by dense brush-like structures, consistent with the morphology of E-cadherin (Fig. 4d). Additionally, we examined tissue sections 18 h after full-thickness skin excision using immunohistochemistry (Fig. 4e and f). The results demonstrate a shared alignment of actin filaments and E-cadherin surrounding the cells in the extended wound epidermis. Unlike the anchored appearance of E-cadherin in the actin cable, the identical distribution of actin filaments and E-cadherin in the actin mesh may be attributed to the sectioning orientation and magnification used. E-cadherin appeared to stabilize the actin mesh over the wound epidermis, creating a sheet-like structure that was observed as a continuous linear pattern in transverse sections rather than as discrete dots.

4. Discussion

The actin cable was first described in the wound-healing process of chick embryos [4]. A purse-string mechanism involving circumferential tension at the free edge of the epithelium appeared to participate in wound contraction. Subsequently, the same mechanism was found in the embryos of mice [5], frogs [6], fruit flies [7], zebrafish [8], adult worms [9], and adult mouse corneas [10]. The shared wound-closure mechanism across different species may indicate an ancient, universal pattern of epithelialization. The

healing process is thought to rely on a complex cytoskeletal network primarily driven by a contractile actin cable around the wound margin. In adult newts, the wound-healing process is initiated by collective cell migration around the wound [3]. Accordingly, we aimed to identify the same mechanism for actin cabling in adult newts. This study demonstrates actin alignment during re-epithelialization. Surprisingly, instead of cables or bundles, a mesh-like structure was identified, which we termed the actin mesh. The actin mesh started from the margin of the wound along the EET and finally covered the wound bed when re-epithelialization was completed. Under SEM, we observed that the EET extended to the wound bed in a sheet pattern, which revealed that the actin mesh maintained the structure of the wound epidermis and overall tension during re-epithelialization. On the other hand, a fiber-rich appearance in the cytoplasm was observed under TEM in EET compared to normal skin, suggesting abundant actin fiber formation during re-epithelialization. It is worth exploring whether this mechanism is conserved in other animals. For instance, *Xenopus* froglets, another amphibian species, exhibit scarless wound-healing abilities and full-thickness skin regeneration in adulthood, including secretory appendages, similar to newts [16]. Additionally, zebrafish demonstrate the ability to regenerate their striped pigmentation patterns after wounding [16]. Investigating whether these species also utilize an actin mesh for achieving scarless skin healing could provide valuable insights into the universality and evolutionary significance of this mechanism.

Initially, it was believed that the actin cable was responsible for scarless healing. However, our findings revealed the presence of the actin mesh in adult newts which plays a crucial role in this process. Therefore, we aimed to compare the differences between the two structures. Research has shown that an actin cable forms at the leading edge of a wound to generate the purse-string contractility necessary for wound closure. As the wound closes, the actin cable gradually shrinks and eventually disappears once the wound is fully closed [17]. In this study, we examined the progression of the actin mesh during the morphological stages of skin regeneration in adult newts. The actin mesh formed at the wound margin alongside the EET eventually covered the wound bed upon the completion of re-epithelialization. Remarkably, this structure persisted for 4–7 days, indicating that it did not dissipate immediately after re-epithelialization was completed. The sustained presence of the actin mesh suggests that it may play additional roles in the later stages of skin regeneration. Previous studies reported that dermal regeneration begins after complete re-epithelialization [3]. This raises the possibility that the prolonged expression of the actin mesh stabilizes the wound epidermis during the critical period of dermal tissue regeneration.

To further investigate the role of the actin mesh in re-epithelialization, we disrupted actin formation using cytochalasin B and monitored the wound healing process. Similar to phalloidins, cytochalasins are natural organic actin-binding molecules [12]. They cap the ends of actin filaments and inhibit polymerization, thereby interfering with actin elongation. In the present study, wounds resulting from full-thickness skin excisions were immersed in a cytochalasin B solution for 1 h. At 18 h postoperation, the EET in the control group displayed a well-formed actin mesh, whereas that in the intervention group showed a remarkable absence of actin fibers. Despite this disruption, there was no observed difference in the wound area in the two groups, and both achieved complete re-epithelialization within 48 h. These results suggest that although cytochalasin B can temporarily disrupt actin mesh formation on the wound surface, it does not appear to affect the overall wound healing timeline. This finding highlights the exceptional regenerative capability of adult newts, which enables

them to complete re-epithelialization even when actin formation is delayed. Experiments involving long-term interference or genetic modification may further explore the effects of impaired actin formation on wound healing and provide deeper insights into the underlying mechanisms.

As we continue to explore the capability of the actin mesh for re-epithelialization, it is important to recognize that wound healing is a complex process involving numerous cytoskeletal molecules. Although the actin mesh may play a central role in re-epithelialization in adult newts, other contributing factors are essential to this process. Re-epithelialization is a dynamic event that occurs during the early stages of wound healing. Adult newts use their rapid re-epithelialization ability to protect the wound bed and reduce granulation tissue formation, ultimately leading to scarless healing [3]. During this process, maintaining the balance of tension within each cell and the overall contractility of the wound epidermis is crucial. According to the “cellular tensegrity” model, F-actin serves as the primary tension-generating element, while myosin provides the necessary contractility [13]. Research has shown that in the formation of the actin cable, myosin is recruited to the innermost region of the wound edge, where it assembles with F-actin to form the actomyosin cable [18]. This contractile ring draws the surrounding cells toward the wound center and maintains stable tension during cell migration, contributing to scarless wound closure. In our study, immunohistochemistry revealed that myosin II was aligned around cells along the wound edge, mirroring the distribution of the actin mesh. We termed this structure the “actomyosin mesh” to differentiate it from the actomyosin cable. Although the mechanical function of this network remains unclear, the alignment of myosin II within the actin mesh suggests its potential role in providing contractility during re-epithelialization. The actomyosin mesh may coordinate cellular movements and force distribution, thereby contributing to scarless wound closure.

Cell-cell junctions also play an important role in the re-epithelialization process by maintaining tissue integrity and organizing the cytoskeleton during wound closure [18]. E-cadherin is a key molecule that facilitates intercellular adhesion and promotes the assembly of the actomyosin cables, driving directional cell migration [19]. Previous research has suggested that the actin cable is partially anchored to the cell membrane through E-cadherin, which helps maintain the tension across the wound epidermis and coordinates cell movement during wound healing [5,14,15]. In the present study, SEM analysis revealed a scale-like pattern over the EET, suggesting the presence of the actin mesh structure beneath the newly formed epidermis. In addition, TEM analysis at a high magnification further demonstrated brush-like structures connecting cells within the wound epidermis, consistent with the morphology of E-cadherin. Immunohistochemical analysis also showed the colocalization of actin filaments and E-cadherin in the extended wound epidermis. E-cadherin functions as an anchor in the actin cable, linking the actin filaments to a purse-string structure that drives wound closure. However, in the actin mesh, E-cadherin appeared to weave together with the actin filaments, creating a complex interconnected surface. Within this network, E-cadherin acts more like a knot, binding strands of the actin mesh and contributing to the stability of the wound epidermis during re-epithelialization. Although the EET is a thin layer, it maintains a sheet-like structure rather than being easily disrupted, although it tends to curl at the margins. Strong intercellular connections facilitated by E-cadherin may be confined to the wound epidermis, which exhibits limited adhesion to the underlying wound bed. This could explain the rapid re-epithelialization observed in adult newts, as the stable expansion of the wound epidermis encounters less resistance from the wound bed, thereby promoting efficient and scarless healing. These findings underscore the complex

interplay between actin, myosin II, and E-cadherin in the formation and stabilization of the actin mesh during re-epithelialization. Further studies regarding the dynamic relationship between the cytoskeleton and cell junctions of newts can help construct a detailed model of the actin mesh.

The present study has several limitations. First, the inherent variability among the animals used in the study resulted in differences in wound size and shape across samples, potentially introducing subtle variations in the timing of re-epithelialization. Second, the intervention targeting actin elongation was limited to a 1 h period through direct local skin contact. This short duration may not fully capture the effects of sustained or systemic interference on actin mesh formation. Further experiments are required to explore the impact of long-term or whole-body interventions, such as genetic engineering, on the dynamics of actin assembly. Third, our observations of myosin and E-cadherin were confined to structural analyses. Because the interaction between these molecules and the actin mesh involves a dynamic equilibrium, additional experimental approaches, such as targeted inhibition of these proteins or genetic engineering, could provide deeper insights into their functional roles and underlying mechanisms. Understanding the temporal stability of these molecules is crucial for elucidating the process of actin mesh construction and maintenance. Future studies should focus on these aspects to refine the current model of actin mesh formation.

The present study demonstrates a distinctive pattern of re-epithelialization mediated by the actin mesh in adult newts. From a clinical perspective, the skin, which is the largest organ in the human body, serves as a critical barrier that protects the internal organs from external stimuli and infections. Upon injury, re-epithelialization is initiated by cell migration toward the wound site, accompanied by cell division at the wound margins. Persistent cell division at the ulcer edges has been observed even when the lesions appeared to be non-healing [20]. This observation suggests that the intractability of chronic skin ulcers is more likely to be owing to a failure in re-epithelialization rather than a deficit in cellular proliferation. Various pathological conditions can impair re-epithelialization. For example, in patients with diabetes mellitus, sustained hyperglycemia induces prolonged systemic inflammatory responses that hinder the wound healing process [21]. Chronic inflammation and infection make diabetic ulcers a considerable burden on patients and healthcare systems worldwide. However, in severe burns, prolonged wound exposure can lead to life-threatening dehydration and substantially increase the risk of infection [22]. Infectious complications can exacerbate inflammation and create a vicious cycle that delays wound healing [23]. Therefore, rapid re-epithelialization is crucial for patients with severe burns to restore the protective skin barrier and to modulate the immune response. The remarkable re-epithelialization capacity of adult newts offers a promising foundation for the development of innovative treatments for chronic wounds. This discovery may redefine therapeutic strategies and pave the way for a new era of innovation in wound care.

Author contributions

Y.L., T.I. designed the study. Y.L., N.M., T.S. and T.I. performed the acquisition of data. Y.L., T.I. and K.K. participated in the analysis and interpretation of the data. Y.L. drafted the manuscript and T.I., K.K. revised the manuscript. All the listed authors approved the final version of the manuscript and have agreed to be personally accountable for the content of this study.

Funding

This work was supported by JSPS KAKENHI (Research registration number: 23H05483). The funding body played no role in the design of the study and collection, analysis, and interpretation of data and in writing the manuscript.

Declaration of competing interest

The authors have no conflicts of interest to report.

Acknowledgments

We thank Chikafumi Chiba for preparing animals, the Japanese fire-bellied newt. We would like to thank Editage (www.editage.jp) for English language editing.

References

- [1] Monavarian M, Kader S, Moeinzadeh S, Jabbari E. Regenerative scar-free skin wound healing. *Tissue Eng Part B Rev* 2019;25:294. <https://doi.org/10.1089/TEN.TEB.2018.0350>.
- [2] Alvarado AS, Tsonis PA. Bridging the regeneration gap: genetic insights from diverse animal models. *Nat Rev Genet* 2006;7(11):873–84. <https://doi.org/10.1038/nrg1923>. 2006;7.
- [3] Ishii T, Takashimizu I, Casco-Robles MM, Taya Y, Yuzuriha S, Toyama F, et al. Skin wound healing of the adult newt, *Cynops pyrrhogaster*: a unique Re-epithelialization and scarless model. *Biomedicines* 2021;9. <https://doi.org/10.3390/Biomedicines9121892/S1>.
- [4] Martin P, Lewis J. Actin cables and epidermal movement in embryonic wound healing. *Nature* 1992;360(6400):179–83. <https://doi.org/10.1038/360179a0>. 1992;360.
- [5] Takaya K, Okabe K, Ishigami A, Imbe Y, Kanazawa H, Sakai S, et al. Actin cable formation and epidermis–dermis positional relationship during complete skin regeneration. *Sci Rep* 2022;12. <https://doi.org/10.1038/S41598-022-18175-Y>.
- [6] Davidson LA, Ezin AM, Keller R. Embryonic wound healing by apical contraction and ingression in *Xenopus laevis*. *Cell Motil Cytoskeleton* 2002;53:163–76. <https://doi.org/10.1002/CM.10070>.
- [7] Kiehart DP, Galbraith CG, Edwards KA, Rickoll WL, Montague RA. Multiple forces contribute to cell sheet morphogenesis for dorsal closure in *Drosophila*. *J Cell Biol* 2000;149:471. <https://doi.org/10.1083/JCB.149.2.471>.
- [8] Hunter MV, Willoughby PM, Bruce AEE, Fernandez-Gonzalez R. Oxidative stress orchestrates cell polarity to promote embryonic wound healing. *Dev Cell* 2018;47:377–387.e4. <https://doi.org/10.1016/J.DEVCEL.2018.10.013>.
- [9] Xu S, Chisholm AD. A Gαq - Ca²⁺ signaling pathway promotes actin-mediated epidermal wound closure in *C. elegans*. *Curr Biol* 2011;21:1960. <https://doi.org/10.1016/J.CUB.2011.10.050>.
- [10] Danjo Y, Gipson IK. Actin ‘purse string’ filaments are anchored by E-cadherin-mediated adherens junctions at the leading edge of the epithelial wound, providing coordinated cell movement. *J Cell Sci* 1998;111:3323–32. <https://doi.org/10.1242/JCS.111.22.3323>.
- [11] Tanaka HV, Ng NCY, Yang Yu Z, Casco-Robles MM, Maruo F, Tsonis PA, et al. A developmentally regulated switch from stem cells to dedifferentiation for limb muscle regeneration in newts. *Nat Commun* 2016;7:11069. <https://doi.org/10.1038/ncomms11069>.
- [12] Cooper JA. Effects of cytochalasin and phalloidin on actin. *J Cell Biol* 1987;105:1473. <https://doi.org/10.1083/JCB.105.4.1473>.
- [13] Boucher E, Goldin-Blais L, Basiren Q, Mandato CA. Actin dynamics and myosin contractility during plasma membrane repair and restoration: does one ring really heal them all? *Curr Top Membr* 2019;84:17–41. <https://doi.org/10.1016/bs.ctm.2019.07.004>. Academic Press Inc.
- [14] Begnaud S, Chen T, Delacour D, Mège R-M, Ladoux B. Mechanics of epithelial tissues during gap closure. *Curr Opin Cell Biol* 2016;42:52–62. <https://doi.org/10.1016/j.ceb.2016.04.006>.
- [15] Danjo Y, Gipson IK. Actin ‘purse string’ filaments are anchored by E-cadherin-mediated adherens junctions at the leading edge of the epithelial wound, providing coordinated cell movement. *J Cell Sci* 1998;111:3323–32. <https://doi.org/10.1242/jcs.111.22.3323>.
- [16] López Lasasa F, Zhou Y, Song J, He Y, Cui Y, Bolea Bailo RM, et al. Nature-inspired scarless healing: guiding biomaterials design for advanced therapies. *Tissue Eng Part B Rev* 2024;30:371–84. <https://doi.org/10.1089/ten.teb.2023.0224>.
- [17] Abreu-Blanco MT, Verboon JM, Liu R, Watts JJ, Parkhurst SM. *Drosophila* embryos close epithelial wounds using a combination of cellular protrusions and an actomyosin purse string. *J Cell Sci* 2012;125:5984–97. <https://doi.org/10.1242/jcs.109066>.
- [18] Rothenberg KE, Fernandez-Gonzalez R. Forceful closure: cytoskeletal networks in embryonic wound repair. *Mol Biol Cell* 2019;30:1353. <https://doi.org/10.1091/MBE18-04-0248>.

- [19] Hunter MV, Lee DM, Harris TJC, Fernandez-Gonzalez R. Polarized E-cadherin endocytosis directs actomyosin remodeling during embryonic wound repair. *JCB (J Cell Biol)* 2015;210:801–16. <https://doi.org/10.1083/jcb.201501076>.
- [20] Adair HM. Epidermal repair in chronic venous ulcers. *Br J Surg* 1977;64: 800–4. <https://doi.org/10.1002/BJS.1800641113>.
- [21] Rodríguez-Rodríguez N, Martínez-Jiménez I, García-Ojalvo A, Mendoza-Mari Y, Guillén-Nieto G, Armstrong DG, et al. Wound chronicity, impaired immunity and infection in diabetic patients. *MEDICC Rev* 2022;24:44–58. <https://doi.org/10.37757/MR2021.V23.N3.8>.
- [22] Roshangar L, Soleimani Rad J, Kheirjou R, Reza Ranjkesh M, Ferdowsi Khosroshahi A. Skin burns: review of molecular mechanisms and therapeutic approaches. *Wounds* 2019;31:308–15.
- [23] Shpichka A, Butnaru D, Bezrukov EA, Sukhanov RB, Atala A, Burdakovskii V, et al. Skin tissue regeneration for burn injury. *Stem Cell Res Ther* 2019;10:94. <https://doi.org/10.1186/s13287-019-1203-3>.